

## Instruments and Methods

# Borehole optical stratigraphy and neutron-scattering density measurements at Summit, Greenland

Robert L. HAWLEY,<sup>1\*</sup> Elizabeth M. MORRIS<sup>2\*</sup>

<sup>1</sup>*Department of Earth and Space Sciences, University of Washington, Seattle, Washington 98195-1310, USA  
E-mail: rlh45@cam.ac.uk*

<sup>2</sup>*British Antarctic Survey, Natural Environment Research Council, Madingley Road, Cambridge CB3 0ET, UK*

**ABSTRACT.** We have made side-by-side measurements in several boreholes at Summit, Greenland, using borehole optical stratigraphy (BOS) and neutron-scattering density logging techniques. The BOS logs show strong positive correlation at shallow depths with neutron-scattering logs taken in the same borehole. This supports the hypothesis that BOS detects changes in density. The positive correlation between returned brightness and density decreases with depth and finally becomes negative. We conclude this inversion of correlation is related to changes in densification regime from grain-boundary sliding to pressure sintering.

### INTRODUCTION

Recent advances in borehole techniques make it possible to measure snow and firn stratigraphy in a borehole, with no need for a core or deep snow pits. Shallow borehole measurements span the range between snow-pit studies and core analyses, in that they can penetrate far deeper than practical for a snow pit, but they can be performed rapidly in the field with no need to transport core to a laboratory for analysis. Borehole measurements can be repeated to assess in situ changes of the properties of firn, and provide a continuous, unbroken record.

Visual stratigraphic measurements have been made extensively in snow pits and on cores for many years. Many different types of layer can be observed, from melt layers to dust or ash layers from a nearby (or sometimes distant) volcanic eruption (Alley and others, 1997). The most readily detectable layering is the 'wind-slab/depth-hoar couplet', which forms the basis of annual-layer counting. This couplet is composed of a layer of low-density, coarse-grained 'depth hoar' overlain by a layer of higher-density, fine-grained 'wind slab'. The depth hoar is formed by thermal-gradient metamorphism in the late summer when strong temperature gradients are present in the upper few decimeters of the snowpack, and the wind slab is formed by winter deposition of wind-blown snow (Alley, 1988). This wind-slab/depth-hoar couplet has been identified with borehole optical stratigraphy (Hawley and others, 2003), and also with the ice geophysical logging system (IGLS) based on the Wallingford neutron probe (Morris and Cooper, 2003).

### METHODS

#### Field location

Summit Camp is a year-round research camp located near the summit of the Greenland ice sheet at  $\approx 72.58^\circ\text{N}$ ,  $38.47^\circ\text{W}$ . It is the site of an ice core drilled 3054 m to bedrock, completed in 1993. The 30 m boreholes used for

this work are approximately 1 km away from the main camp. The mean annual temperature at Summit is  $-31^\circ\text{C}$  and the mean accumulation is  $\approx 25\text{ cm a}^{-1}$  (ice equivalent) (Meese and others, 1994; Alley and Woods, 1996).

#### Field measurements

##### *Borehole optical stratigraphy*

Borehole optical stratigraphy (BOS) has been developed as a technique for simple and rapid measurement of vertical strain in a borehole. The equipment and processing involved in creating a BOS profile are described in detail by Hawley (2005). In essence, a borehole video camera is used to obtain similar information to that observed by visual stratigraphers on a core. The downward-looking, wide-angle video camera is connected to the surface by a three-conductor cable which carries both video signal and power. A portable DV camcorder at the top of the hole allows the operator to view and record the log. The depth of the camera is measured with an optical encoder mounted on the shaft of the pulley over which the cable runs into the hole. This depth is then written in the upper left corner of the video screen. In post-processing, an annulus of pixels around the borehole wall is sampled and the mean intensity of these pixels is recorded. At the same time, the depth is read from the frame using optical character recognition. The field time required for a log is minimal (less than 30 min for a 30 m log, including set-up and take-down). The end product of the BOS process is a log of light intensity vs depth.

##### *Neutron-scattering density probe*

The density probe used for this experiment was a version of the Wallingford soil-moisture probe, adapted for use in measuring snow density as part of an IGLS (Morris and Cooper, 2003). The probe consists of an annular radioactive source of fast neutrons around a cylindrical detector of slow neutrons. Fast neutrons are emitted from the source. As they move through the snow, they lose energy by scattering. The count rate of slow neutrons arriving back at the detector per unit time is related to the density of the snow.

A calibration equation based on three-group scattering theory relates count rate to the density of the surrounding

\*Present address: Scott Polar Research Institute, University of Cambridge, Lensfield Road, Cambridge CB2 1ER, UK.

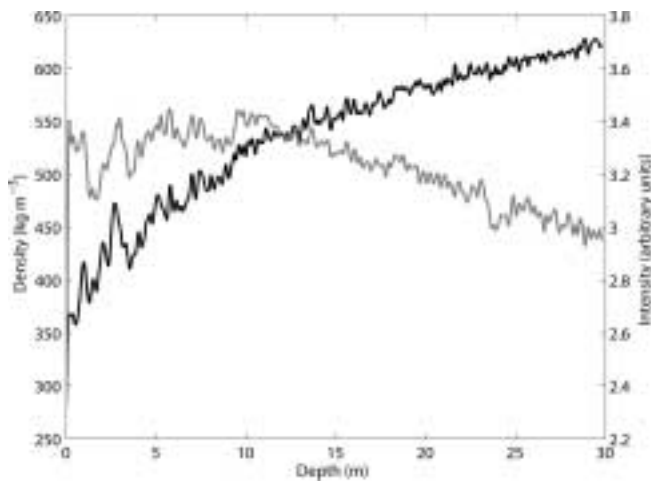


**Fig. 1.** The density and optical profiles. Density is the black line and intensity is the grey line. Several features can be seen that are replicated in the two logs, particularly in the shallow region.

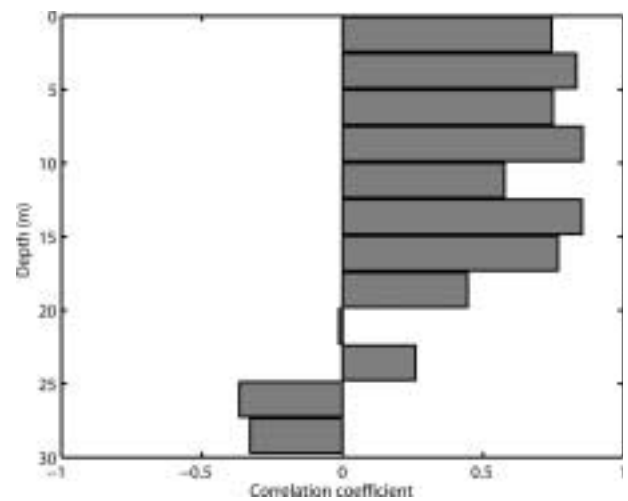


**Fig. 2.** Windowed correlations between density and intensity. At shallow depths, correlation is excellent, but deeper it fades. See Discussion for details.

medium, given the borehole diameter and distance from the wall of the borehole (degree of centralization). Errors in the density can arise from deviations from the nominal borehole diameter and deviation from the nominal degree of centralization. These errors can be reduced if the actual borehole diameter is measured as a function of depth using calipers and if the neutron probe is held in position, either using a centralizer, or using a spring device to hold it against the wall of the borehole.

The emission of fast neutrons is a random process, so the relative error in the count rate decreases with a lengthened counting period and with increased source strength. Using a radioactive source small enough to be easily manageable in

the field, logging speeds of  $\approx 2 \text{ cm min}^{-1}$  are required for cm-scale detail. In this case we use a speed of  $7 \text{ cm min}^{-1}$ . The result of an IGLS log is a profile of density as a function of depth. Figure 1 shows the two logs plotted together.

## DATA REDUCTION

### Filtering and correlation

We low-pass filtered all logs with a length-scale cut-off of 10 cm to remove the effect of high-frequency noise. We calculated the correlation coefficient between the logs in windows of approximately 2.5 m to assess the correlation

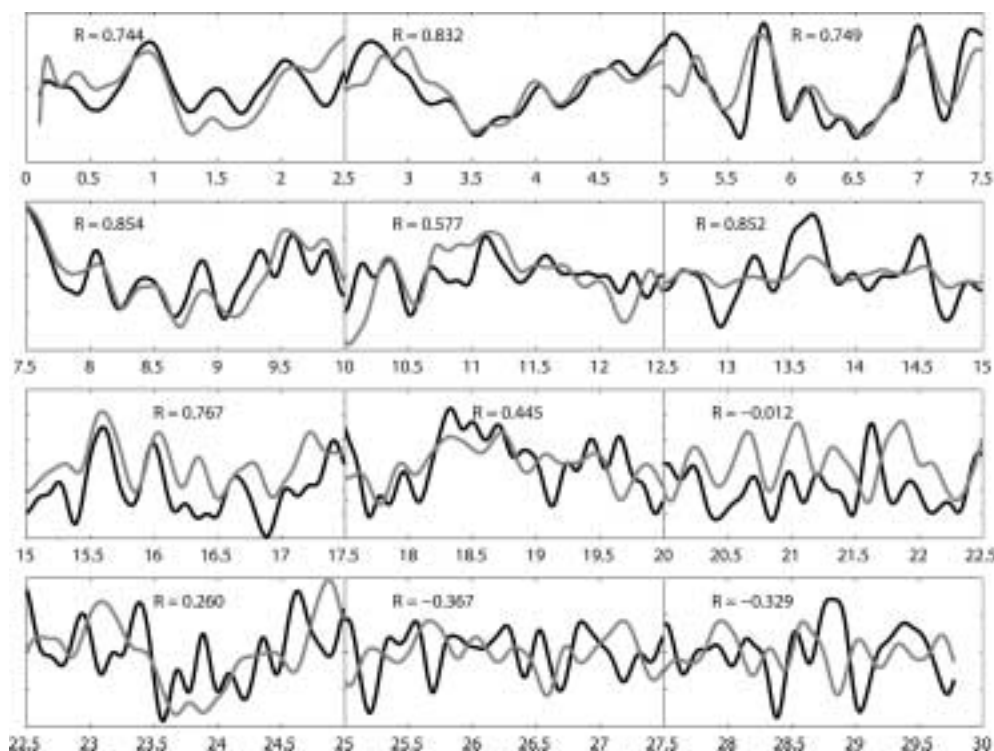


**Fig. 3.** Windows for correlation. The data in each window are de-trended and scaled for display. Density is shown as a black line and intensity is shown in grey. The correlation coefficient for each window is shown. Depth in meters increases along the horizontal axis.

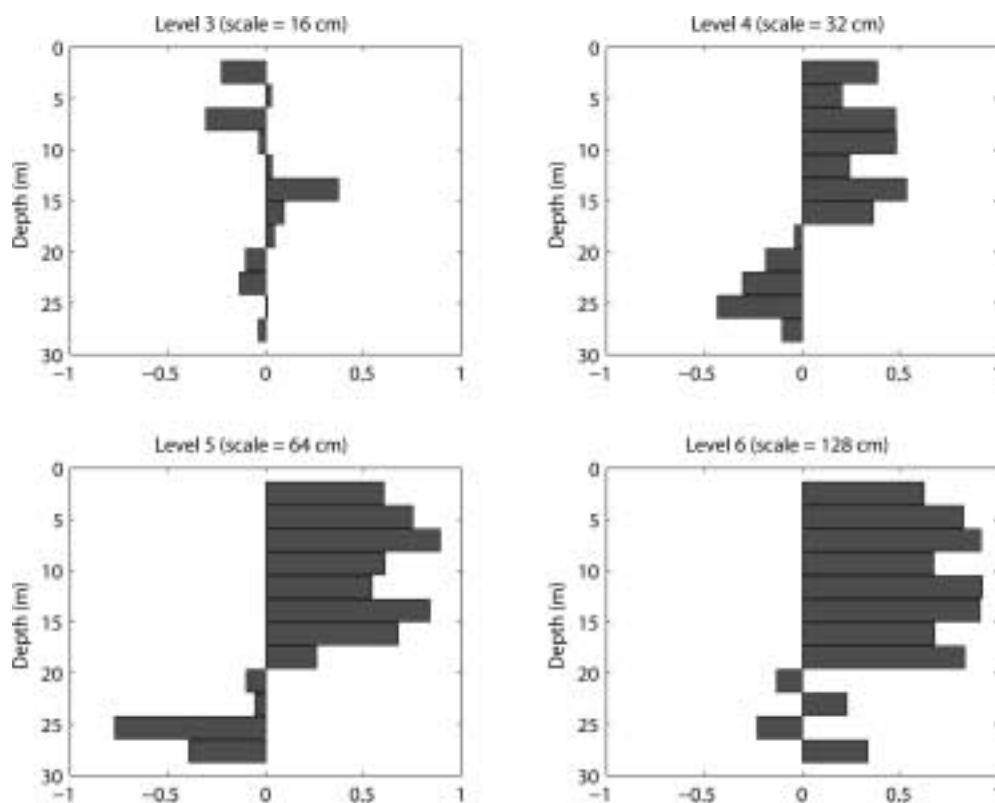


**Fig. 4.** Windowed correlation between wavelet coefficients at four different scales. Below level 4, no real pattern in correlation is seen. At levels 4–6 a pattern of decreasing correlation with depth is observed, which becomes significantly negative at levels 4 and 5. This increases our confidence in the trend of the correlation.

between logs using different methods. These ‘windowed’ correlation coefficients are shown in Figure 2 and the data from each window are shown in Figure 3. As can be seen in Figure 2, the correlation is strongly positive near the surface; however, it decreases and finally becomes negative near the bottom of the borehole (approximately 30 m).

### Wavelet correlation

Simple windowed correlation of the two datasets may fail to show some relationships between them if the data are non-stationary, as would be expected for annual layers, where layer thickness decreases with depth due to compaction. The size of the window chosen for correlation might then have a direct impact on the types of relationship shown by the analysis. This possibility was addressed by turning to wavelet methods, which naturally accommodate non-stationary data. As an alternative method for determining the scale-dependent correlation between two datasets, the correlation between wavelet coefficients at selected scales can be used (Whitcher and others, 2000; Cornish and others, 2006).

A wavelet transform decomposes a data series into a series of wavelet coefficients which represent the ‘power’ the original series contains for a given shape and scale of the original wavelet. Correlations between the wavelet coefficients at a given scale for two series can expose or reinforce relationships that were not seen in standard filtering or Fourier analysis. We wished to determine whether the ‘inversion of correlation’ that is seen in the simple windowed correlation is a robust feature of the data.

Following Cornish and others (2006), the maximal overlap discrete wavelet transform (MODWT) was used on each dataset. For each wavelet scale, we calculated the

same windowed correlation between the two sets of wavelet coefficients. We found the most meaningful correlations at wavelet scale 5, which corresponds to a scale of roughly 64 cm in our data. Furthermore, at level 5, the correlation follows the same trend as our filtered data, having a positive correlation near the surface, dropping through zero to a significantly negative correlation at the bottom of the hole. Figure 4 shows windowed correlations at wavelet scales 3–6.

### Reconciling depth measurement errors

Since the BOS and IGLS logging systems are independent, using different methods to measure depth, a depth calibration is needed to compare logs performed with the two systems. Since the BOS depth measurement was designed with precision rather than accuracy in mind, we assumed the IGLS depths are accurate and that the BOS depths require calibration. The two systems have different measuring systems, cables with different properties, and different pulleys. The basic form of the transform from original BOS depth  $z$  to IGLS depth  $z^*$  is  $z^* = mz$ . To determine  $m$  we chose two ‘landmark packets’ of features, one near the surface and one around 15 m, which were of the same shape in each log and were clearly the same features. We varied  $m$  to align the logs in the deeper region, ensuring also that they did not become misaligned in the shallow region. Our best value of  $m$  was 0.99. Figure 5 shows the two sets of features we used for this calibration.

We might produce the correlation pattern discussed in previous subsections if density and returned brightness were actually positively correlated through the entire depth of our survey, and if some part of our depth calibration was

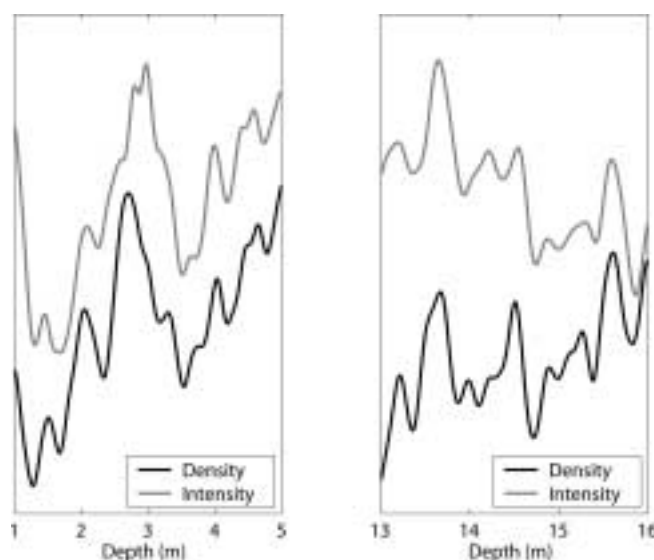


**Fig. 5.** The two sets of ‘landmark packets’ used to co-register the two logs.

incorrectly calculated or if one cable stretched during the experiment. If we went deep enough, or if the stretch was great enough, the correlation would become positive again. The length scale of features for which we see the strongest correlation and anticorrelation are in the order of 15–25 cm, so a differential stretch of 7–12 cm or approximately 0.2–0.5% could produce this result. Both cable stretch and calibration errors would manifest themselves in a linear way; by varying the linear multiplier  $m$  we should be able to test and see whether we return to an all positive correlation with another multiplier. Figure 6 shows the result of varying the linear multiplier  $m$  by 1% on each side of our preferred value. Note that the decrease in correlation with depth appears to be a robust result. The strongest overall correlations are seen at and near our preferred value of  $m$ . Thus we believe we do not have a stretching cable or spurious calibration problem.

## DISCUSSION

As Figures 2–4 show, we find a positive correlation between density and returned brightness in the shallow region (0–15 m) of our survey. Also evident is that the correlation fades to near zero and becomes negative in the deeper reaches of the survey (20–30 m). In this section we discuss the possible reasons for this pattern of correlation.

### Density

The transformation of snow into ice takes place under at least three distinct regimes with different physical processes contributing to compaction. In regime 1 ( $\approx 0.3$ – $0.55 \text{ g cm}^{-3}$ , from the surface to about 15 m at Summit), densification takes place primarily by grain-boundary sliding (Alley, 1987). This mechanism ceases to be dominant when the relative density of snow approaches that of random close-packed spheres; that is, all of the ice grains have moved to a point where they are supported on all sides by other ice grains. In regime 2 ( $\approx 0.55$ – $0.8 \text{ g cm}^{-3}$ ), further densification then takes place by pressure sintering, during which the contact bonds between grains thicken and the interstices between the grains become smaller (Arthern and Wingham, 1998). Eventually,

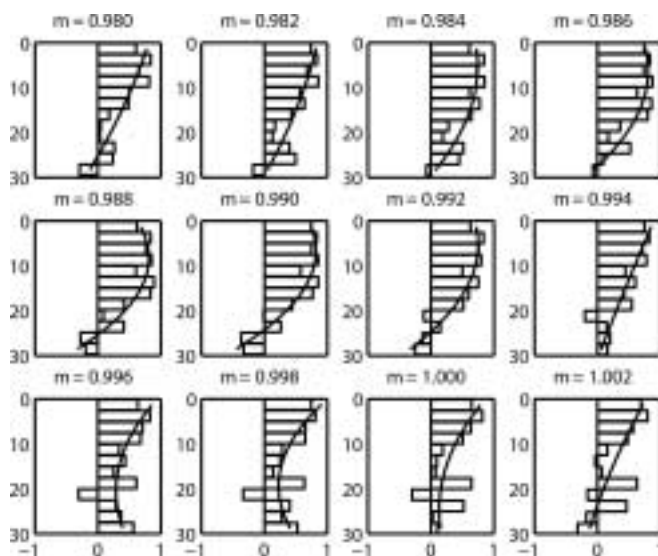


**Fig. 6.** Windowed correlations under scenarios of differing cable stretch. We span our preferred  $m$  value of 0.99 and calculate the correlations if the cable were stretching or contracting. Note that the reduction in correlation with depth is a robust feature of the data.

the interstices become isolated from one another; this transition is known as ‘pore close-off’. In regime 3 ( $\approx 0.8$ – $0.92 \text{ g cm}^{-3}$ ), the confining pressure is resisted by bubble pressure in the sealed air bubbles.

In snow, firn or ice, the amount of light returned to the borehole camera is dominated by the amount of scattering in the material. At visible wavelengths, absorption is minimal. To first order, scattering is determined by the cross-sectional area of scatterers. In the shallow regions we are concerned with here, the primary scatterer of photons is the interface between air and ice. When there is more air–ice interface surface area per unit volume, there will be more scattering.

In regime 1, densification takes place primarily by grain-boundary sliding. If no changes in grain shape occur, this process will bring more scattering surface area into a unit volume as density increases, resulting in more scattering and greater returned brightness in the borehole log. In regime 2, further densification is by pressure sintering, which involves thickening the necks between grains and producing more rounded shapes. This process is partially driven by surface energy effects and destroys surface area, so as the firn gets denser in regime 2, there is less scattering surface area per unit volume, which decreases the returned brightness in the video log. The positive correlation begins to drop as the change between regimes 1 and 2 is reached ( $\approx 15$  m). This implies that the same factors that influence dominant densification mechanisms (increasing grain co-ordination number, changing grain and pore geometry) are also responsible for this change in relationship between brightness and density.

### Grain size and shape

Grain size and shape play an important role in scattering at visible wavelengths. At a constant density a smaller grain size results in more scattering surface area, and thus a greater backscattered intensity. Larger grain size has the opposite effect. Grain shape also has an effect on scattering surface area: a sphere is the solid shape with the lowest

surface:volume ratio, so as grains become more spherical they lose scattering surface area and scattering decreases.

Several modeling studies (Bohren and Barkstrom, 1974; Wiscombe and Warren, 1980; Warren, 1982) have shown the effect of grain size in radiative transfer, so we expect that returned brightness is indicative of grain size. Two important complications prevent us from attempting a simple correlation study between grain size and returned brightness. The most important complication is that grain shape, in addition to grain size, is very important in scattering. Grenfell and Warren (1999) showed that for any shape of snow grain, the important dimension for visible light scattering is the average path a photon takes through the grain, which, with most grain shapes, is close to the shortest path. The second most important and related complication arises from uncertainties in reporting of grain size. For example with depth-hoar 'plate-like' grains, the thickness of such a grain is the important dimension for scattering, whereas the diameter of the grain is likely to be reported.

### Grain-size–density correlation

Bohren and Beschta (1979) noted that, since grain size and density are often covariant, it is difficult to distinguish their contributions to radiative transfer. Near the surface at Summit, high-density fine-grained winter snow alternates with low-density large-grained summer surface hoar. Since both increasing density and decreasing grain size should lead to increasing returned brightness, the correlation between density and grain size reinforces, or could even be the sole cause of, the apparent correlation between optical brightness and density. Grain size and density would need to become anticorrelated to produce the negative correlations between brightness and density we see below 20 m.

### Density 'inversion'

Gerland and others (1999) noted that variations in the density of a core collected at Berkner Island, Antarctica, appeared to undergo an 'inversion of correlation' with electrical conductivity (ECM) measurements on the core. Above 25 m, the peaks in density were anticorrelated with peaks in ECM (interpreted as summer peaks), and were correlated below 25 m. A modeling study by Li and Zwally (2002) found that initially lower-density late-spring and summer snow reached higher densities than late-fall and winter snow. Other studies in snow pits and shallow cores (e.g. Shoji and Langway, 1989) have found the reverse to be true: higher densities correspond with winter signals in the isotope record even deeper in the core. Chemical analysis of another core from our site (personal communication from J.R. McConnell) shows that such a 'density inversion' does not occur at our site.

### CONCLUSIONS AND FUTURE WORK

We have measured co-registered, high-resolution, in situ profiles of density and optical brightness at Summit. The positive correlation between the two logs is high at shallow depths and decreases with depth, becoming significantly negative near the bottom of the borehole at 30 m. While we cannot determine uniquely the relationship between returned brightness, density and grain size, we believe that the change to negative correlation between the logs arises at the transition between grain-boundary sliding and pressure sintering as the dominant firn densification mechanism.

There are several steps that we can take to further our understanding of this process. A deeper survey would allow us to determine whether the negative correlation observed near the bottom of the hole is sustained. A laboratory study would also help to shed light on this issue, by measuring density, grain size and returned brightness on firn cores.

### ACKNOWLEDGEMENTS

This work was financially supported by the US National Science Foundation under grants OPP-0352584 and OPP-0335330, and by the UK Natural Environment Research Council under grant NER/O/S/2003/00620. We thank VECO Polar Resources (R. Abbott, K. Young, P. Adkins, M. Flanagan, K. Hess and T. Wood) and G. Somers for support in the field. The boreholes for this project were drilled by Ice Core Drilling Services, and we thank drillers J. Kyne and B. Bergeron for their excellent work. We thank G. Lamorey for field assistance and providing us with density data from the cores. Many fruitful discussions with E. Waddington, D. Winebrenner, S. Warren and A. Rasmussen improved this work. Finally, we thank D. Fisher, an anonymous reviewer and D. Peel (Scientific Editor) for thoughtful reviews that improved the manuscript.

### REFERENCES

- Alley, R.B. 1987. Firn densification by grain-boundary sliding: a first model. *J. Phys. [Paris]*, **48**, Colloq. C1, 249–254. (Supplément au 3.)
- Alley, R.B. 1988. Concerning the deposition and diagenesis of strata in polar firn. *J. Glaciol.*, **34**(118), 283–290.
- Alley, R.B. and G.A. Woods. 1996. Impurity influence on normal grain growth in the GISP2 ice core, Greenland. *J. Glaciol.*, **42**(141), 255–260.
- Alley, R.B. and 11 others. 1997. Visual-stratigraphic dating of the GISP2 ice core: basis, reproducibility, and application. *J. Geophys. Res.*, **102**(C12), 26,367–26,382.
- Athern, R.J. and D.J. Wingham. 1998. The natural fluctuations of firn densification and their effect on the geodetic determination of ice sheet mass balance. *Climatic Change*, **40**(4), 605–624.
- Bohren, C.F. and B.R. Barkstrom. 1974. Theory of the optical properties of snow. *J. Geophys. Res.*, **79**(30), 4527–4535.
- Bohren, C.F. and R.L. Beschta. 1979. Snowpack albedo and snow density. *Cold Reg. Sci. Technol.*, **1**(1), 47–50.
- Cornish, C.R., C.S. Bretherton and D.B. Percival. 2006. Maximal overlap wavelet statistical analysis with application to atmospheric turbulence. *Bound.-Layer Meteorol.*, **119**(2), 339–374.
- Gerland, S., H. Oerter, J. Kipfstuhl, F. Wilhelms, H. Miller and W.D. Miners. 1999. Density log of a 181 m long ice core from Berkner Island, Antarctica. *Ann. Glaciol.*, **29**, 215–219.
- Grenfell, T.C. and S.G. Warren. 1999. Representation of a nonspherical ice particle by a collection of independent spheres for scattering and absorption of radiation. *J. Geophys. Res.*, **104**(D24), 31,697–31,709.
- Hawley, R.L. 2005. Borehole investigations of firn processes. (PhD thesis, University of Washington.)
- Hawley, R.L., E.D. Waddington, R.A. Alley and K.C. Taylor. 2003. Annual layers in polar firn detected by Borehole Optical Stratigraphy. *Geophys. Res. Lett.*, **30**(15), 1788. (10.1029/2003GL017675.)
- Li, J. and H.J. Zwally. 2002. Modeled seasonal variations of firn density induced by steady-state surface air-temperature cycle. *Ann. Glaciol.*, **34**, 299–302.
- Meese, D.A. and 8 others. 1994. The accumulation record from the GISP2 core as an indicator of climate change throughout the Holocene. *Science*, **266**(5191), 1680–1682.

- Morris, E.M. and J.D. Cooper. 2003. Instruments and methods. Density measurements in ice boreholes using neutron scattering. *J. Glaciol.*, **49**(167), 599–604.
- Shoji, H. and C.C. Langway, Jr. 1989. Physical property reference horizons. In Oeschger, H. and C.C. Langway, Jr, eds. *The environmental record in glaciers and ice sheets*. Chichester, etc., John Wiley and Sons, 161–175.
- Warren, S.G. 1982. Optical properties of snow. *Rev. Geophys. Space Phys.*, **20**(1), 67–89.
- Whitcher, B., P. Guttorp and D.B. Percival. 2000. Wavelet analysis of covariance with application to atmospheric time series. *J. Geophys. Res.*, **105**(D11), 14,941–14,962.
- Wiscombe, W.J. and S.G. Warren. 1980. A model for the spectral albedo of snow. I. Pure snow. *J. Atmos. Sci.*, **37**(12), 2712–2733.

*MS received 18 January 2006 and accepted in revised form 24 August 2006*